



OPEN

A finite element analysis of relationship between fracture, implant and tibial tunnel

Yiqun Wang^{1,5}, Erpeng Qi^{1,5}, Xiaojun Zhang², Lu Xue³, Lianyou Wang^{4,5}✉ & Jiahe Tian^{2,5}✉

The purpose of this article was to use finite element analysis (FEA) to study the relationship of tibial tunnel (TT) with fracture pattern and implants. A computed tomography scan of full-length tibia and fibula was obtained. Models were built after three-dimensional reconstruction. The corresponding plates and screws were constructed and assembled together with fracture models. FEA was performed and contourplots were output. The Von Mises stresses of nodes and displacements of elements were extracted. Student's t test was used to compare the values of Von Mises stresses and displacements between corresponding models. Differences in Von Mises stresses and displacements of fragments and implants between models with and without TT were nearly all statistically significant. However, the displacements of fragments and implants for all models were < 2 mm. TT in fracture models had larger Von Mises stresses than TT in intact tibial model. However, displacements of TT in fracture models showed similar or even smaller results to those in intact tibial model. Although almost all the tested parameters were statistically significant, differences were small and values were all below the clinical threshold. This study could promote open reduction and internal fixation with one-stage reconstruction for treatment of tibial plateau fractures associated with anterior cruciate ligament (ACL) ruptures.

Tibial plateau fractures (TPF) account for about one-tenth of tibial fractures¹, and isolated anterior cruciate ligament (ACL) injuries account for almost half of knee ligament injuries². When both occur simultaneously, it presents a very difficult situation for orthopaedists.

Avulsed fractures of ACL should be reattached in one-stage³. As for TPF associated with ACL ruptures, it is commonly accepted that ACL should undergo two-stage reconstruction³⁻⁶. Why not reconstruct ACL in one-stage procedure? In 1978, Schatzker et al.³ concluded in their article that “the collateral ligaments are more important than the anterior cruciate, and for the sake of early mobilization we would be prepared to sacrifice an anterior cruciate and carry out a late reconstruction if necessary”. However, this concept has been challenged by the in-depth studies. Early reconstruction of ACL can provide a nurturing environment for the healing of medial collateral ligament (MCL)⁷. An MCL-deficient knee may still be stabilized by remaining structures, particular ACL⁸. For most combined ACL/MCL injuries, reconstruction of the ACL alone can achieve good clinical results⁷⁻⁹.

Other views against one-stage reconstruction included that early reconstruction would cause further soft tissue damage to an already injured knee. But with the advancement of technology for soft tissue protection, these problems have gradually been overcome^{10,11}. Bennett and Browner⁴ believed that obtaining bone-patellar tendon-bone graft would interfere with the fracture pattern. Currently, both hamstring and peroneus longus autografts^{12,13} and allografts¹⁴ have achieved good clinical outcomes.

Meanwhile, two-stage reconstruction has limitations. Some studies had indicated that the most unsatisfactory outcomes of TPF were due to the anterior instability^{3,5,10,11}. Two-stage reconstruction has a high incidence of meniscus injury, which leads to secondary changes of the bone and joint¹⁵ and at least 1-year loss in activity, which also leads to a reduction bone mineral density in the knee¹⁶.

However, balancing the relationship of tibial tunnel (TT), a conduit that contains and fixes the ACL graft, with fracture and implants is challenging. Many accepted opinions believe that implants will restrict TT and the

¹Medical School of Chinese PLA, Chinese PLA General Hospital, Beijing, China. ²Department of Nuclear Medicine, Chinese PLA General Hospital, 28 Fuxing Road, Beijing, China. ³Department of Orthopaedics, Tianjian Hospital, Tianjin, China. ⁴Department of Pathology, China-Japan Union Hospital of Jilin University, No. 126 Xiantai Street, Changchun, Jilin, China. ⁵These authors contributed equally: Yiqun Wang, Erpeng Qi, Lianyou Wang and Jiahe Tian. ✉email: 644657124@qq.com; www9299sss@163.com

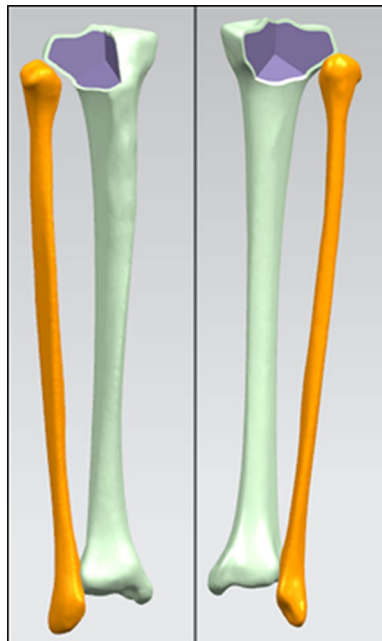


Figure 1. Lateral and posterior column fracture models (created by Solidworks 2018, <https://www.solidworks.com/zh-hans>).

strength of TT will be insufficient due to the fracture. Nonetheless, there is a lack of available literature specifically demonstrating the infeasibility of one-stage reconstruction.

Finite element analysis (FEA) has been used in orthopaedics for more than two decades and considered as an optimization technique to guide clinical decision-making and to effectively predict the displacement and stress of object under load¹⁷. In the present study, FEA was used to explore whether the presence of fracture and implants will weaken and restrict the TT.

Materials and methods

This study was approved by the institutional review board of Chinese People's Liberation Army General Hospital and in accordance with the ethical standards of Declaration of Helsinki. Written informed consent was provided for the study. A female (age: 23 years 7 months old, height: 171 cm, weight: 57 kg) was enrolled with no previous history of fracture or osteoarthritis, and an average weekly activity level of > 2 h. A computed tomography (CT) scan with 0.5-mm full-length tibia and fibula was obtained.

The CT data were imported into Mimics (Materialize Company, Leuven, Belgium) in Digital Imaging and Communications in Medicine (DICOM) format and then reconstructed in three-dimensional images. Next, the model was input into the Geomagic Studio 2013 (Geomagic, Research Triangle Park NC, USA) in STL format and smoothing, wrapping and segmenting cortical and cancellous bone were defined. A rough measurement of the cortical bone thickness of about 2–4 mm was obtained from the CT scan, thus, cortical bone thickness was set to be 2 mm artificially.

Next, the above model was imported into Solidworks 2018 (Dassault Systemes Simulia Corp., Providence, RI, USA) in STEP format. The construction of fracture models was based on the “three-column fixation” theory¹⁸. On the cross section, the tibial plateau was divided in three parts through three lines connecting the three points on the edge of the tibial plateau to the center. One point should be noticed that in article of Luo et al., they use the line from the center of the knee to the most anterior point of the fibular head to separate the lateral and posterior columns¹⁸. However, through a traditional anterolateral arc incision, the fibular head could be exposed by stripping the upper rear region¹⁹. Herein, the line from the center of the knee to the posterolateral ridge of the proximal tibia (at approximately the center of the fibular head) was used to separate the lateral and posterior column. As no data available about the thickness of tibial plateau or readymade lateral or posterior column fracture model, so the upper edge of the superior tibiofibular joint (TFJ) was set as the initial plane, three-column connecting lines were made and the bottom of the lateral and posterior fracture surface traversed the tibia at the bottom edge of superior TFJ, then the lateral column fracture (LCF) model, posterior column fracture (PCF) model, and lateral-posterior column fracture (LPCF) model consisting of two fragments were created (Fig. 1).

Next, a cylinder, 1-cm in diameter, was built to simulate TT. The cylinder was positioned at the plane of midpoint between tibial tuberosity and posteromedial ridge and the exit was located slightly behind ACL tibial insertion to prevent interference with the intercondylar roof. The shortest distance between the cylinder and the LCF was about 1 mm and that between the TT and the PCF was about 2 mm. Intact tibia with the TT (ITTT), LCF with the TT (LCFTT), PCF with the TT (PCFTT), and LPCF with the TT (LPCFTT) models were obtained

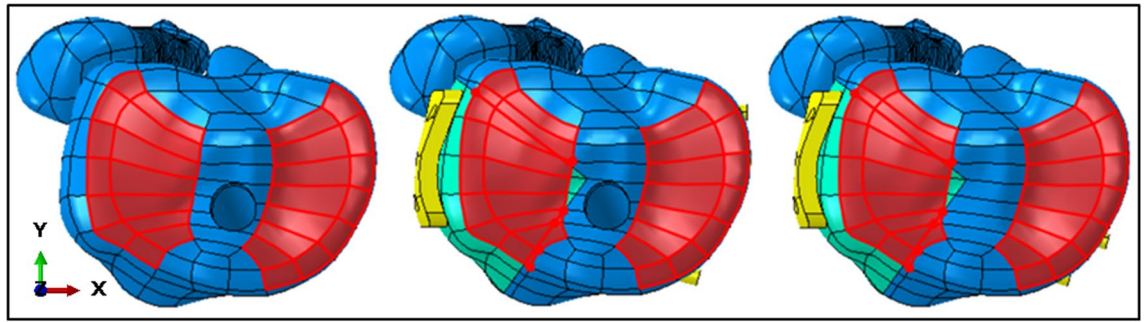


Figure 2. Load area of ITTT, fracture models with tibial tunnel and fracture models without tibial tunnel (take lateral column fracture as an example, created by Abaqus 6.14, <https://www.3ds.com/zh/products-services/simulia/products/abaqus/>).

through original models subtracting aforementioned cylinder to simulate the condition that open reduction and internal fixation in a one-stage ACL reconstruction surgery for the treatment of tibial plateau fracture.

Plates were constructed using bone surfaces and their isometric offset surfaces cutting the solid extrude of plates to simulate complete fits of plates and models. Screws were modeled using cylinders with a diameter of 3.5 mm. As for the LCF and LCFTT, inverted L-shaped plates (80 mm in height, 30 mm in length, 10 mm in width, 4 mm in thickness) were used. Three screws were used in the plateau plane. For the LCF, plateau screws were arranged in parallel, while for LCFTT, the last two screws were adjusted backward by 15° simulating pol-axial screw^{20,21}.

T-shaped plates (height: 80 mm, length: 40 mm, width: 10 mm, thickness: 4 mm) were used for PCF and PCFTT. The position of plate was slightly lowered due to the posterior tibial slope angle. Four screws were used in plateau plane. For the PCF, plateau screws were arranged in parallel, while for the PCFTT, the inner two screws were slightly adjusted inward. As for the LPCF and LPCFTT, the two plates and the plateau screws were combined. All plates had one buttress screw and two distal screws.

The models were input into Abaqus 6.14 (Dassault Systemes Simulia Corp., Providence, RI, USA). Implants, including plates and screws, were simulated Ti6Al4V. Both implants and bone were assumed elastic, linear, and composed of isotropic materials. The elastic modulus of cortical bone, cancellous bone, and implant were 13GPa, 126 MPa, 114GPa respectively, and the respective Poisson's ratios were 0.30, 0.30, and 0.34^{22–24}. The fibula was bonded within the area of proximal tibia of non-fractured bone by multi-point constraints. The distal part of tibia and fibula was fixed without displacement. Friction coefficient between fragments was 0.4²⁵ and that between screws and cancellous bone was 0.8. Screws were fixed to cortical bone by sharing the same nodes of elements. The plate was bonded with screws by mimicking locking compression plate and contact surface between plate and bone was assumed to be smooth (see Supplemental Table 1 for all the connection).

The load area was set as the size of a concave formed by connecting line between anterior and posterior horn of medial and lateral meniscus (Fig. 2). 60% force was applied on the medial compartment, and 40% force on the lateral. 80 kg bipedal static standing position was simulated, indicating that a single plateau could withstand about 340 N ($80 \text{ kg} \times 9.8 \text{ N/kg} \times 85.6\% \times 0.5$)^{23,26}.

For ease of convergence and calculation, tetrahedral four-node elements were used to mesh bones and plates; tetrahedral eight-node elements with reduced integration were used to mesh screws. Element size was three. There were refinements between screws and holes and there was no sharp discontinuity leading to unrealistically high stress concentration. A mesh verification analysis was performed and showed the satisfactory results.

All jobs were submitted and the corresponding plot contours were output. Bearing the capacity and elastic modulus of cortical and cancellous bone are apparently different, they should not be analyzed as a whole as their Von Mises stresses will vary widely. Since cortical bone strength was significantly higher than that of cancellous bone and in clinical situation, as for failure of TT, most of these cases were due to the collapse of the cancellous bone, for this reason, so only the cancellous bone was analyzed here. If external force causes a fracture through TT, it is a completely different matter and were not included in this study. The plate and the screws were analyzed as a whole. For the accuracy of stress and displacement analysis, Von Mises stress on the nodes and displacement on the elements were extracted and the extracted data were the difference before and after the application of force. Since stress and displacement are vectors, all the x-axis (from right to left), y-axis (from anterior to posterior), z-axis (from bottom to top) and absolute values were analyzed (axis of the coordinate system was showed in Fig. 2).

Statistical analysis. Von Mises stress and displacement were expressed as the mean \pm standard deviation. The Student's t test was used to compare Von Mises stresses and displacements of cancellous bone and implants between corresponding models and of TT between ITTT and matching fracture models with TT. All tests were 2-tailed and p-value < 0.05 was regarded as statistically significant. All statistical analyses were performed using GraphPad Prism 8.0.2 (GraphPad Software, San Diego, CA, USA).

Ethical review committee statement. This study was approved by the institutional review board.

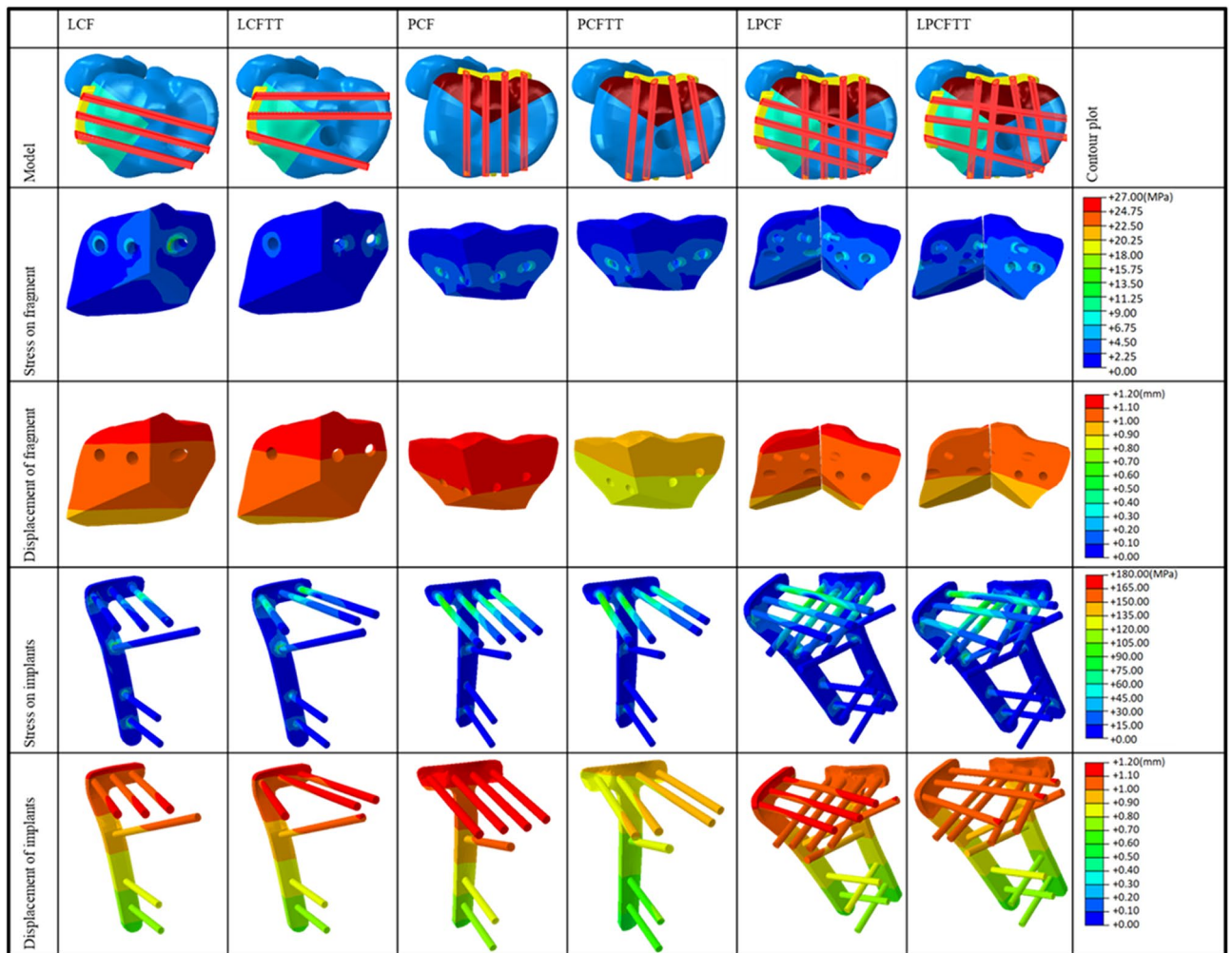


Figure 3. Corresponding plot contours of Von Mises stress and displacement of fragment and implants between fracture models with and without TT and deformation scale factor for each model was uniform and the value of it was ten (created by Abaqus 6.14, <https://www.3ds.com/zh/products-services/simulia/products/abaqus/>).

Results

Corresponding contourplots and data of Von Mises stresses and displacements of fragment and implants were shown in Fig. 3 and Table 1. The numbers of extracted nodes and elements are shown in parentheses inside table. Almost all differences in parameters used to compare models with TT and matching models without TT were statistically significant. However, differences between matching models were minimal and displacements of fragments of all models were < 2 mm. Besides, fragment displacement of PCFTT and LPCFTT showed even smaller results than corresponding models. Displacement of implants also had similar performance.

In terms of stresses on fragments, all models without TT showed lower stresses than those of corresponding models with TT, but their differences were also small. As for stress concentration, no fracture models with TT showed significant stress concentration, however LCF showed a slightly stress concentration located at the junction between last plateau screw and fracture line with a maximum of 27.5 MPa. The stress applied on implants showed the same phenomenon.

Corresponding contourplots and data of Von Mises stresses and displacements of TT were shown in Fig. 4 and Table 2. For stress parameters, the values of TT in fracture models were almost one order of magnitude higher than those in ITTT. The maximum Von Mises stress of TT in ITTT was 0.45 MPa, located in trailing edge of entrance of TT. The maximum of LCFTT was 8.62 MPa, located in outer edge of exit of TT. The maximum of PCFTT was 8.54 MPa, located in trailing edge of exit of TT. Maximum of LPCFTT was 5.50 MPa, located in posterosuperior part of TT. However, displacements showed completely different phenomenon than stresses. There were no statistically significant differences in displacement of TT between ITTT and LCFTT ($p = 0.062$). Displacement of TT in PCFTT and LPCFTT showed smaller results than that of ITTT.

The stress of TT in fracture models were also compared with the stress of fragments in corresponding fracture models without TT and data dispersion was shown in Fig. 5. Except the mean stress values of TT in LCFTT was

	Lateral		Posterior		Lateral-Posterior	
	LCF	LCFTT	PCF	PCFTT	LPCF	LPCFTT
Stress on fragment (x-axis)	-0.06±0.84	-1.38±0.67	-0.82±0.58	-0.78±0.60	-0.61±0.73	-0.81±0.85
Stress on fragment (y-axis)	-0.60±0.57	-0.70±0.62	-1.57±0.79	-1.58±0.86	-1.12±0.83	-1.06±0.93
Stress on fragment (z-axis)	-0.68±0.59	-0.38±0.87	0.22±1.17	0.28±1.24	0.19±1.25	0.28±1.40
Stress on fragment (absolute)	1.52±1.21 (39,390)	1.91±0.02 (37,102)	2.68±1.07 (27,889)	2.79±1.12 (25,495)	2.59±1.12 (78,310)	2.76±1.19 (68,609)
Displacement of fragment (x-axis)	0.56±0.01	0.55±0.02	0.59±0.02	0.48±0.02	0.56±0.02	0.53±0.02
Displacement of fragment (y-axis)	-0.92±0.02	-0.94±0.02	-0.94±0.01	-0.75±0.01	-0.90±0.03	-0.88±0.02
Displacement of fragment (z-axis)	0.00±0.04	0.01±0.04	-0.00±0.04	-0.01±0.03	0.00±0.05	0.00±0.05
Displacement of fragment (absolute)	1.08±0.02 (7696)	1.09±0.02 (7273)	1.12±0.02 (5649)	0.90±0.02 (5195)	1.06±0.03 (16,079)	1.03±0.02 (14,813)
Stress on implants (x-axis)	5.68±11.91	8.92±15.33	-0.79±4.99	-0.48±4.69	4.83±13.64	4.33±12.98
Stress on implants (y-axis)	-0.18±6.07	0.03±5.70	10.57±19.30	15.66±22.79	5.41±15.19	8.82±18.79
Stress on implants (z-axis)	0.62±10.24	0.54±9.79	-1.42±8.27	-1.76±7.41	0.15±9.62	-0.03±9.04
Stress on implants (absolute)	12.38±11.17 (10,524)	15.31±14.04 (11,344)	17.26±17.32 (12,776)	22.17±20.74 (17,091)	17.58±16.95 (24,975)	19.87±18.59 (28,921)
Displacement of implants (x-axis)	0.51±0.08	0.51±0.08	0.52±0.09	0.44±0.06	0.51±0.08	0.49±0.07
Displacement of implants (y-axis)	-0.86±0.10	-0.88±0.10	-0.88±0.11	-0.73±0.07	-0.84±0.10	-0.83±0.09
Displacement of implants (z-axis)	-0.04±0.08	-0.04±0.08	-0.06±0.08	-0.05±0.06	-0.05±0.08	-0.05±0.08
Displacement of implants (absolute)	1.00±0.13 (6856)	1.02±0.13 (8626)	1.03±0.14 (9057)	0.85±0.09 (13,674)	0.99±0.13 (18,440)	0.97±0.11 (22,907)

Table 1. Von Mises stress and displacement of cancellous fragment and implants of fracture models with and without TT. The content inside parentheses was the number of extracted nodes or elements. Data were expressed as mean ± standard deviation. The values of fracture models with TT were compared with corresponding models without TT. The unit of stress and displacement is MPa and mm respectively. The data of corresponding models were not statistically significant or the models with TT were statistically significant ($P < 0.05$) from the matching models without TT were shown in italics.

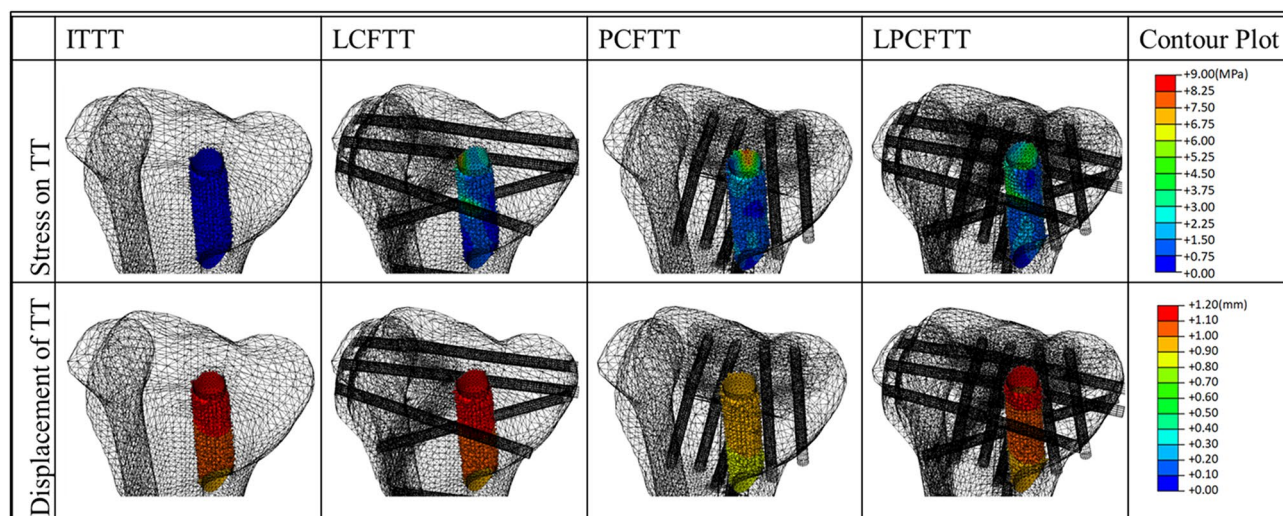


Figure 4. Corresponding plot contours of Von Mises stress and displacement of TT and deformation scale factor for each model was uniform and the value of it was one (created by Abaqus 6.14, <https://www.3ds.com/zh/products-services/simulia/products/abaqus/>).

higher than that of fragment in LCF (about 0.17 MPa), the mean stress values of TT in other two type were all lower than those of fragments in corresponding fracture models without TT.

	ITTT	LCFTT	PCFTT	LPCFTT
Stress (x-axis)	0.01 ± 0.06	- 0.16 ± 0.83	0.69 ± 1.98	- 0.72 ± 0.88
Stress (y-axis)	- 0.00 ± 0.03	0.83 ± 1.61	- 0.13 ± 0.67	- 0.46 ± 0.78
Stress (z-axis)	- 0.17 ± 0.09	0.30 ± 0.78	0.10 ± 0.69	0.51 ± 0.87
Stress (absolute)	0.21 ± 0.07 (1402)	1.69 ± 1.33 (1402)	1.82 ± 1.33 (1305)	2.05 ± 1.13 (1374)
Displacement (x-axis)	0.56 ± 0.04	<i>0.55 ± 0.03</i>	<i>0.47 ± 0.03</i>	<i>0.53 ± 0.04</i>
Displacement (y-axis)	- 0.92 ± 0.05	- <i>0.93 ± 0.05</i>	- <i>0.78 ± 0.04</i>	- <i>0.89 ± 0.05</i>
Displacement (z-axis)	- 0.13 ± 0.02	- <i>0.13 ± 0.02</i>	- <i>0.11 ± 0.02</i>	- <i>0.12 ± 0.03</i>
Displacement (absolute)	1.08 ± 0.06 (735)	<i>1.09 ± 0.06 (735)</i>	<i>0.92 ± 0.05 (686)</i>	<i>1.04 ± 0.06 (721)</i>

Table 2. Von Mises stress and displacement of TT between ITTT and fracture models with TT. The content inside parentheses was the number of extracted nodes or elements. Data were expressed as mean ± standard deviation. The values of the fracture models with TT were compared with those of ITTT. $P < 0.05$ and the better results of each fracture models are indicated as italics.

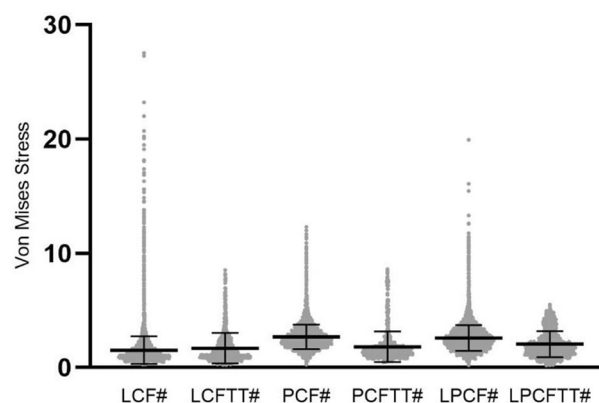


Figure 5. Data dispersion of absolute values of Von Mises stress between TT in fracture model with TT and fragment corresponding fracture model without TT. The unit of Von Mises stress is MPa. LCF# means the stress of fragment of LCF, LCFTT# means the stress of TT in LCFTT, PCF# means the stress of fragment of PCF, PCFTT# means the stress of TT in PCFTT, LPCF# means the stress of fragment of LPCF, LPCFTT# means the stress of TT in LPCFTT.

Discussion

To our knowledge, this is the first article in English literature that evaluate the relationship of TT with fracture pattern and implants and we found that although nearly all data were statistically significant, the differences were small and all data were lower than their clinical threshold, which could support ORIF with one-stage reconstruction for treatment of TPF associated with ACL ruptures.

It has frequently been sustained at conferences that TPF associated with ACL rupture is uncommon. What is the incidence of TPF associated with ACL rupture? The Segond fracture strongly suggested ACL rupture with a positive predictive value between 71 and 100%^{27,28}. Peltola et al.²⁸ reported 23 TPF with Segond fractures, of which 17.4% were associated with complete ACL rupture. In a report describing 39 TPF, eight were associated with ACL injuries⁵, although the type of injury was not described, the authors concluded that the prognosis of TPF associated with cruciate ligament injury was often poor. Thirty cases of TPF were described in which three cases presented ACL injuries, of which one was a mid-substance injury⁴. A further 20 reported cases of non-displaced and minimally displaced TPF indicated that two were ACL ruptures²⁹. Of 103 cases of TPF subjected to surgery, half of the patients showed an ACL partial tear and 11% had complete tear on MRI analysis³⁰. There may not be a large number of TPF associated with ACL rupture, but it is not uncommon and treatment has a decisive influence on patient prognosis.

In a report of 64 lateral tibial plateau occult fracture, half had ACL ruptures³¹. Using MRI on 100 patients with complete ACL tears, Kaplan et al. reported that approximately all had posterolateral occult TPF³². A further description of 10 patients with posteromedial TPF showed all were accompanied by ACL tears³³ and in 25 reported cases of posterolateral TPF, 80% of which with ACL tears³⁴. Common mechanisms of ACL rupture include excessive anterior displacement of tibia relative to femur and internal rotation and valgus of knee^{35,36}. When force is continuous or too large, theoretically, lateral, posterior or posterolateral TPF will occur, which is also the basis for model-building.

In this study, differences in displacement and stress values of cancellous bone of fragment and implants between models with and without TT were nearly all statistically significant, however, the differences were small and each displacement and stress value was below the clinical threshold, which indicated that displacement of

fragment was < 2 mm¹⁷ and stress of implants was < 2800 MPa²². In our case, statistically significant did not necessarily mean clinically significant, thus the above results should not be a reason to avoid one-stage reconstruction.

Displacement and stress of TT in ITTT were compared with those in LCFTT, PCFTT, and LPCFTT. The resulting stress of corresponding models was statistically significant with differences of about one order of magnitude. However, the displacement of TT in fracture models showed the same or smaller results than ITTT. Generally, the relationship between displacement and stress should be linear. We think this situation is due to the load weight on TT combined with the simultaneous load generated by support screws and fixed fragment, based on forces of action and reaction, which was responsible for maintaining the shape of TT and the load generated by support screws was larger than that between cancellous bone and that explains why displacements of PCFTT and LPCFTT were smaller than that of ITTT.

Although limited information is available about the strength of TT, the ultimate strength of proximal tibia has been reported as 5.3 ± 2.9 MPa³⁷ and the shear strength of lateral tibial plateau cancellous bone may vary from 2.4 to 5.8 MPa³⁸. Using electrical measurements, the yield stress of medial tibial plateau was predicted to be 9.0 ± 3.7 MPa³⁹. Although the values given above intersects with data reported in our article, our data showed that stress on TT in fracture models was generally smaller than that on fragment in corresponding fracture models and this is not necessary for full-weight bearing for ORIF or reconstruction in early stages. Following a complete and personalized rehabilitation program, the statistical significance of stress applied on TT should also not be considered a reason to prevent one-stage reconstruction of ACL. Double-tunnel ACL reconstruction has improved its effectiveness⁴⁰. Considering only 1–2 mm between the two tunnels, why could not one-stage reconstruction be performed.

Feasibility of ORIF with one-stage reconstruction for LCF, PCF, and LCPF associated with ACL rupture has been discussed in this study. Isolated medial TPF associated with ACL rupture is very rare. When it occurs, because the plate requires placement either medially or antero-medially, and thus is not recommended for one-stage reconstruction. As for medial column fractures, which involve a break in medial column wall¹⁸, these can usually be classified as Schatzker IV, V, VI, and in some circumstances can undergo one-stage reconstruction. In a case of Schatzker V and knee dislocation that also presented ACL, posterior cruciate ligament (PCL) rupture as well as posterolateral corner injury were treatment by ORIF with one-stage reconstruction⁴¹. Surgical details, however, were not described. We previously reported a Schatzker VI fracture with a Segond fracture, presenting a fracture line through the medial column. MRI demonstrated a complete proximal ACL rupture and a chronic avulsion of PCL⁴². Because the soft tissue envelope of medial tibial plateau is thin and an anterolateral plate was already present, in that case, posterior plate showed superior biomechanical advantages⁴³, thus a posteromedial plate was applied, which successfully fixed the medial column fracture.

Bearing capacity of cortical and cancellous bone is apparently different, they should not be analyzed as a whole. Since cortical bone strength was Some orthopaedists may be discouraged by the placement of forefront screw of LCFTT. Indeed, the distance between TT and anterior edge of tibial is about 1.5 cm^{2,40}, which is sufficient to place a screw. If conditions permit, an experienced and skilled orthopaedist and computer navigation could make the process simple.

As for TPF associated with ACL rupture, we can imagine that the injured limb is very swollen and requires calcaneus traction or external fixation to reduce edema for 1–2 weeks. Reconstruction of < 1 week increased the likelihood of arthrofibrosis compared with reconstruction of > 3 weeks⁴⁴, however, a further study⁴⁵ reported that the injury to surgery time was not related to the timing of surgery. In addition to the latter, the occurrence of arthrofibrosis of knee is also associated with soft tissue damage surrounding the knee, graft choice, surgical technique, postoperative rehabilitation, and genetics. Given the numerous uncertainties, long standing disputes will remain for a consensus on arthrofibrosis⁴⁶.

ACL was not simulated in this study because its stiffness was low and did not strongly impact the results. For TT fixation, cross-pin fixation is a safe method but the position of screws needs to be considered, while interference screw fixation does not require consideration of the position of screws but is somewhat risky. Other methods are available, but deserve further study.

This article has similar limitations to those of similar nature. In our study, bone was presume to be an isotropic, linear, elastic material and screws were replaced by cylinders, which is a time-saving and feasible method^{47,48}. Although it has been reported that the elastic modulus can be calculated by average CT value⁴⁹, results reported by different studies are inconsistent^{50,51}, in addition, the Poisson's ratio and the association between bone and screws in recent studies still refer to previous reports, which were not specific. Then we assigned a friction coefficient of 0.8 to the surface between screws and cancellous bone which was first proposed in a study of the friction coefficient between bead-surfaced metals and tibial cancellous bone⁵². However, the density and the strength of cortical and cancellous bone differ and friction coefficients should not be simply approximated. Here a term which is commonly used in mechanics and architecture was involved-pretightening force. In our bone-implant system, when screws are fixed to the holes of plate and cortical bone, it can be considered equivalent to the fixation of nuts and bolts. Under no pressure, the interface will produce pretightening force, which is related to material properties, thread and tightening torque. Tightening torque between the hole of cortical bone and screw could be envisioned as the screw being fastened into the cortical bone after tapping and the bone would have a tendency to rebound after being tightened. When the interface is subjected to pressure, the pretightening force is mainly generated by mutual compression between the surrounding bone and the screws. This is the basic theory that the dynamic compression plate can stabilize the fracture. So, we combined the above-mentioned concepts and defined the contact between cortical bone and screws as fixed together.

Then, FEA is a simulation study and if a validation experiment can be performed, it will likely increase the credibility of results.

Next, artificially segmented fracture models and perfect fit between plate and bone do not represent the actual clinical situation. And distribution of screws may differ from case to case.

Finally, only one CT data was enrolled and only bipedal static standing position was simulated. Although increasing the number of CT data may somewhat reduce the effect of geometry differences on results, yet it is not necessary for full weight bearing or walking immediately after surgery and partial weighting or non-weighting will make the results in this article more reliable without the need for additional CT data, in addition the numbers of extracted nodes and elements are more than several thousands, slight differences would make statistically significant, but it did not represent clinically significant. Above all, the purpose of this study was to provide a new clinical insight for treating TPF associated with ACL rupture rather treatment of a specific case.

Conclusions

This study explored the relationship between TT and fracture patterns and implants. As for stress and displacement of cancellous bone of fragments and implants of models with and without TT, although most differences in evaluated parameters were statistically significant, differences were small and below the clinical threshold. As for TT, although the differences in stress between three corresponding models were approximately one order of magnitude, the differences in displacement of three corresponding model were similar. Following a complete and personalized rehabilitation program, ORIF with one-stage reconstruction for the treatment of TPF associated with ACL rupture can be considered a feasible method. As for orthopaedists, the principles of AO and BO for fracture treatment and the concepts and techniques of sports medicine are equally important. Only by allowing ourselves to keep improving can we provide better benefit to patients.

Received: 10 March 2020; Accepted: 6 January 2021

Published online: 19 January 2021

References

- Burri, C., Bartzke, G., Coldewey, J. & Muggler, E. Fractures of the tibial plateau. *Clin. Orthop. Relat. Res.* **138**, 84–93 (1979).
- Zantop, T., Wellmann, M., Fu, F. H. & Petersen, W. Tunnel positioning of anteromedial and posterolateral bundles in anatomic anterior cruciate ligament reconstruction: Anatomic and radiographic findings. *Am. J. Sports Med.* **36**, 65–72. <https://doi.org/10.1177/0363546507308361> (2008).
- Schatzker, J., McBroom, R. & Bruce, D. The tibial plateau fracture. The Toronto experience 1968–1975. *Clin. Orthop. Relat. Res.* **138**, 94–104 (1979).
- Bennett, W. F. & Browner, B. Tibial plateau fractures: A study of associated soft tissue injuries. *J. Orthop. Trauma* **8**, 183–188 (1994).
- Delamarter, R. B., Hohl, M. & Hopp Jr, E. Ligament injuries associated with tibial plateau fractures. *Clin. Orthop. Relat. Res.* **250**, 226–233 (1990).
- Honkonen, S. E. Indications for surgical treatment of tibial condyle fractures. *Clin. Orthop. Relat. Res.* **302**, 199–205 (1994).
- Woo, S. L. *et al.* The effects of transection of the anterior cruciate ligament on healing of the medial collateral ligament. A biomechanical study of the knee in dogs. *J. Bone Joint Surg.* **72**, 382–392 (1990).
- Millett, P. J., Pennock, A. T., Sterett, W. I. & Steadman, J. R. Early ACL reconstruction in combined ACL-MCL injuries. *J. Knee Surg.* **17**, 94–98 (2004).
- Azar, F. M. & Aaron, D. G. Jr. Surgical treatment of anterior cruciate ligament-posterior cruciate ligament-medial side knee injuries. *J. Knee Surg.* **18**, 220–227 (2005).
- Abdel-Hamid, M. Z. *et al.* Arthroscopic evaluation of soft tissue injuries in tibial plateau fractures: Retrospective analysis of 98 cases. *Arthroscopy* **22**, 669–675. <https://doi.org/10.1016/j.arthro.2006.01.018> (2006).
- Halinen, J., Lindahl, J., Hirvensalo, E. & Santavirta, S. Operative and nonoperative treatments of medial collateral ligament rupture with early anterior cruciate ligament reconstruction: A prospective randomized study. *Am. J. Sports Med.* **34**, 1134–1140. <https://doi.org/10.1177/0363546505284889> (2006).
- Kerimoglu, S., Kosucu, P., Livaoglu, M., Yukunc, I. & Turhan, A. U. Magnetic resonance imagination of the peroneus longus tendon after anterior cruciate ligament reconstruction. *Knee Surg. Sports Traumatol. Arthrosc.* **17**, 35–39. <https://doi.org/10.1007/s00167-008-0626-7> (2009).
- Samuelsen, B. T., Webster, K. E., Johnson, N. R., Hewett, T. E. & Krych, A. J. Hamstring autograft versus patellar tendon autograft for ACL reconstruction: Is there a difference in graft failure rate? A meta-analysis of 47,613 patients. *Clin. Orthop. Relat. Res.* **475**, 2459–2468. <https://doi.org/10.1007/s11999-017-5278-9> (2017).
- Bait, C., Randelli, P. & Compagnoni, R. Italian consensus statement for the use of allografts in ACL reconstructive surgery. *Knee Surg. Sports Traumatol. Arthrosc.* **27**, 1873–1881. <https://doi.org/10.1007/s00167-018-5003-6> (2019).
- Daniel, D. M. *et al.* Fate of the ACL-injured patient. A prospective outcome study. *Am. J. Sports Med.* **22**, 632–644. <https://doi.org/10.1177/036354659402200511> (1994).
- van Meer, B. L. *et al.* Bone mineral density changes in the knee following anterior cruciate ligament rupture. *Osteoarthr. Cartil.* **22**, 154–161. <https://doi.org/10.1016/j.joca.2013.11.005> (2014).
- Anderson, D. D. *et al.* Computational techniques for the assessment of fracture repair. *Injury* **45**(Suppl 2), S23–31. <https://doi.org/10.1016/j.injury.2014.04.005> (2014).
- Luo, C. F., Sun, H., Zhang, B. & Zeng, B. F. Three-column fixation for complex tibial plateau fractures. *J. Orthop. Trauma* **24**, 683–692. <https://doi.org/10.1097/BOT.0b013e3181d436f3> (2010).
- Hu, S. J. *et al.* The anterolateral supra-fibular-head approach for plating posterolateral tibial plateau fractures: A novel surgical technique. *Injury* **47**, 502–507. <https://doi.org/10.1016/j.injury.2015.11.010> (2016).
- Biggi, E., Di Fabio, S., D'Antimo, C. & Trevisani, S. Tibial plateau fractures: Internal fixation with locking plates and the MIPO technique. *Injury* **41**, 1178–1182. <https://doi.org/10.1016/j.injury.2010.08.001> (2010).
- Cullen, A. B., Curtiss, S. & Lee, M. A. Biomechanical comparison of polyaxial and uniaxial locking plate fixation in a proximal tibial gap model. *J. Orthop. Trauma* **23**, 507–513. <https://doi.org/10.1097/QAI.0b013e3181a25368> (2009).
- ASTM F136 "Standard specification for wrought titanium-6aluminum-4vanadium ELI (extra low interstitial) alloy for surgical implant applications (UNS R56401)".
- Goldstein, S. A., Wilson, D. L., Sonstegard, D. A. & Matthews, L. S. The mechanical properties of human tibial trabecular bone as a function of metaphyseal location. *J. Biomech.* **16**, 965–969. [https://doi.org/10.1016/0021-9290\(83\)90097-0](https://doi.org/10.1016/0021-9290(83)90097-0) (1983).
- Guo, X. Mechanical properties of cortical bone and cancellous bone tissue. In *Bone Mech. Handb.* 2nd edn (2001).
- Rüedi, T. P., Buckley, R. I. & Moran, C. G. *AO Principles of Fracture Management* 2nd edn. (AO publishing, Geneva, 2007).
- Maquet, P. *Biomechanics of the Knee: With Application to the Pathogenesis and the Surgical Treatment of Osteoarthritis.* 2nd edn. (1984).

27. Dietz, G. W., Wilcox, D. M. & Montgomery, J. B. Second tibial condyle fracture: Lateral capsular ligament avulsion. *Radiology* **159**, 467–469. <https://doi.org/10.1148/radiology.159.2.3961179> (1986).
28. Peltola, E. K., Mustonen, A. O., Lindahl, J. & Koskinen, S. K. Second fracture combined with tibial plateau fracture. *AJR Am. J. Roentgenol.* **197**, W1101–1104. <https://doi.org/10.2214/ajr.10.6095> (2011).
29. Shepherd, L., Abdollahi, K., Lee, J. & Vangsness, C. T. Jr. The prevalence of soft tissue injuries in nonoperative tibial plateau fractures as determined by magnetic resonance imaging. *J. Orthop. Trauma* **16**, 628–631. <https://doi.org/10.1097/00005131-200210000-00003> (2002).
30. Gardner, M. J. *et al.* The incidence of soft tissue injury in operative tibial plateau fractures: A magnetic resonance imaging analysis of 103 patients. *J. Orthop. Trauma* **19**, 79–84. <https://doi.org/10.1097/00005131-200502000-00002> (2005).
31. Rosen, M. A., Jackson, D. W. & Berger, P. E. Occult osseous lesions documented by magnetic resonance imaging associated with anterior cruciate ligament ruptures. *Arthroscopy* **7**, 45–51. [https://doi.org/10.1016/0749-8063\(91\)90077-b](https://doi.org/10.1016/0749-8063(91)90077-b) (1991).
32. Kaplan, P. A. *et al.* Occult fracture patterns of the knee associated with anterior cruciate ligament tears: Assessment with MR imaging. *Radiology* **183**, 835–838. <https://doi.org/10.1148/radiology.183.3.1584943> (1992).
33. Chan, K. K., Resnick, D., Goodwin, D. & Seeger, L. L. Posteromedial tibial plateau injury including avulsion fracture of the semi-membranous tendon insertion site: Ancillary sign of anterior cruciate ligament tear at MR imaging. *Radiology* **211**, 754–758. <https://doi.org/10.1148/radiology.211.3.r99jn16754> (1999).
34. Wang, Y., Cao, F., Liu, M., Wang, J. & Jia, S. Incidence of soft-tissue injuries in patients with posterolateral tibial plateau fractures: A retrospective review from 2009 to 2014. *J. Knee Surg.* **29**, 451–457. <https://doi.org/10.1055/s-0036-1581132> (2016).
35. Koga, H. *et al.* Mechanisms for noncontact anterior cruciate ligament injuries: Knee joint kinematics in 10 injury situations from female team handball and basketball. *Am. J. Sports Med.* **38**, 2218–2225. <https://doi.org/10.1177/0363546510373570> (2010).
36. Salem, H. S. *et al.* Contact versus noncontact anterior cruciate ligament injuries: Is mechanism of injury predictive of concomitant knee pathology?. *Arthroscopy* **34**, 200–204. <https://doi.org/10.1016/j.arthro.2017.07.039> (2018).
37. Linde, F. & Hvid, I. The effect of constraint on the mechanical behaviour of trabecular bone specimens. *J. Biomech.* **22**, 485–490. [https://doi.org/10.1016/0021-9290\(89\)90209-1](https://doi.org/10.1016/0021-9290(89)90209-1) (1989).
38. Carrera, I. *et al.* Fixation of a split fracture of the lateral tibial plateau with a locking screw plate instead of cannulated screws would allow early weight bearing: A computational exploration. *Int. Orthop.* **40**, 2163–2169. <https://doi.org/10.1007/s00264-015-3106-y> (2016).
39. Sierpowska, J. *et al.* Prediction of mechanical properties of human trabecular bone by electrical measurements. *Physiol. Meas.* **26**, S119–S131. <https://doi.org/10.1088/0967-3334/26/2/012> (2005).
40. Adachi, N. *et al.* Reconstruction of the anterior cruciate ligament. Single- versus double-bundle multistranded hamstring tendons. *J. Bone Joint Surg.* **86**, 515–520 (2004).
41. Stannard, J. P., Wilson, T. C., Volgas, D. A. & Alonso, J. E. Fracture stabilization of proximal tibial fractures with the proximal tibial LISS: Early experience in Birmingham, Alabama (USA). *Injury* **34**(Suppl 1), A36–42. [https://doi.org/10.1016/s0020-1383\(03\)00256-0](https://doi.org/10.1016/s0020-1383(03)00256-0) (2003).
42. Wang, Y., Wang, L., Zhu, T., Liu, Z. & Liu, G. Open reduction and internal fixation in a one-stage anterior cruciate ligament reconstruction surgery for the treatment of tibial plateau fractures: A case report and literature review. *Injury* **49**, 1215–1219. <https://doi.org/10.1016/j.injury.2018.03.015> (2018).
43. Zeng, Z. M., Luo, C. F., Putnis, S. & Zeng, B. F. Biomechanical analysis of posteromedial tibial plateau split fracture fixation. *Knee* **18**, 51–54. <https://doi.org/10.1016/j.knee.2010.01.006> (2011).
44. Shelbourne, K. D., Wilckens, J. H., Mollabashy, A. & DeCarlo, M. Arthrofibrosis in acute anterior cruciate ligament reconstruction. The effect of timing of reconstruction and rehabilitation. *Am. J. Sports Med.* **19**, 332–336. <https://doi.org/10.1177/036354659101900402> (1991).
45. Beynonn, B. D., Johnson, R. J., Abate, J. A., Fleming, B. C. & Nichols, C. E. Treatment of anterior cruciate ligament injuries, part I. *Am. J. Sports Med.* **33**, 1579–1602. <https://doi.org/10.1177/0363546505279913> (2005).
46. Magit, D., Wolff, A., Sutton, K. & Medvecky, M. J. Arthrofibrosis of the knee. *J. Am. Acad. Orthop. Surg.* **15**, 682–694 (2007).
47. Brown, C. J., Sinclair, R. A., Day, A., Hess, B. & Procter, P. An approximate model for cancellous bone screw fixation. *Comput. Methods Biomech. Biomed. Eng.* **16**, 443–450. <https://doi.org/10.1080/10255842.2011.624516> (2013).
48. Inzana, J. A., Varga, P. & Windolf, M. Implicit modeling of screw threads for efficient finite element analysis of complex bone-implant systems. *J. Biomech.* **49**, 1836–1844. <https://doi.org/10.1016/j.jbiomech.2016.04.021> (2016).
49. Chen, P. *et al.* Newly designed anterolateral and posterolateral locking anatomic plates for lateral tibial plateau fractures: A finite element study. *J. Orthop. Surg. Res.* **12**, 35. <https://doi.org/10.1186/s13018-017-0531-1> (2017).
50. Mulder, L., van Rietbergen, B., Noordhoek, N. J. & Ito, K. Determination of vertebral and femoral trabecular morphology and stiffness using a flat-panel C-arm-based CT approach. *Bone* **50**, 200–208. <https://doi.org/10.1016/j.bone.2011.10.020> (2012).
51. Pahr, D. H. & Zysset, P. K. Finite element-based mechanical assessment of bone quality on the basis of in vivo images. *Curr. Osteoporos. Rep.* **14**, 374–385. <https://doi.org/10.1007/s11914-016-0335-y> (2016).
52. Rancourt, D., Shirazi-Adl, A., Drouin, G. & Paiement, G. Friction properties of the interface between porous-surfaced metals and tibial cancellous bone. *J. Biomed. Mater. Res.* **24**, 1503–1519. <https://doi.org/10.1002/jbm.820241107> (1990).

Acknowledgements

We deeply thank Mr. Lei Zhang and Mr. Zenghai Xia for their careful instruction.

Author contributions

Y.Q.W. wrote the original draft, X.J.Z. run the data curation and formal analysis, E.P.Q. and L.X. used the softwares, L.Y.W. was supervision and designed the project, J.H.T. was supervision and reviewed and edited the draft.

Competing interests

The authors declare no competing interests.

Additional information

Supplementary Information The online version contains supplementary material available at <https://doi.org/10.1038/s41598-021-81401-6>.

Correspondence and requests for materials should be addressed to L.W. or J.T.

Reprints and permissions information is available at www.nature.com/reprints.

Publisher's note Springer Nature remains neutral with regard to jurisdictional claims in published maps and institutional affiliations.



Open Access This article is licensed under a Creative Commons Attribution 4.0 International License, which permits use, sharing, adaptation, distribution and reproduction in any medium or format, as long as you give appropriate credit to the original author(s) and the source, provide a link to the Creative Commons licence, and indicate if changes were made. The images or other third party material in this article are included in the article's Creative Commons licence, unless indicated otherwise in a credit line to the material. If material is not included in the article's Creative Commons licence and your intended use is not permitted by statutory regulation or exceeds the permitted use, you will need to obtain permission directly from the copyright holder. To view a copy of this licence, visit <http://creativecommons.org/licenses/by/4.0/>.

© The Author(s) 2021